

**On the Mechanism of the Palladium(II)-Catalyzed  
Decarboxylative Olefination of Arene Carboxylic Acids.  
Crystallographic Characterization of Non-Phosphine  
Palladium(II) Intermediates and Observation of Their Stepwise  
Transformation in Heck-like Processes**

Daisuke Tanaka, Stuart P. Romeril, and Andrew G. Myers\*

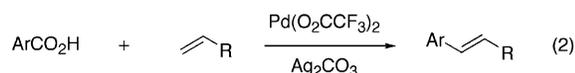
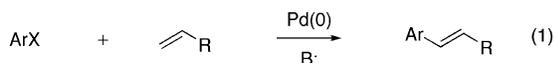
*Contribution from the Department of Chemistry and Chemical Biology, Harvard University,  
Cambridge, Massachusetts 02138*

Received April 1, 2005; E-mail: myers@chemistry.harvard.edu

**Abstract:** Mechanistic studies of a palladium-mediated decarboxylative olefination of arene carboxylic acids are presented, providing spectroscopic and, in two instances, crystallographic evidence for intermediates in a proposed stepwise process. Sequentially, the proposed pathway involves carboxyl exchange between palladium(II) bis(trifluoroacetate) and an arene carboxylic acid substrate, rate-determining decarboxylation to form an arylpalladium(II) trifluoroacetate intermediate (containing two trans-disposed *S*-bound dimethyl sulfoxide ligands in a crystallographically characterized form), then olefin insertion and  $\beta$ -hydride elimination. Because of the unique mode of generation of the arylpalladium(II) trifluoroacetate intermediate, a species believed to be substantially electron-deficient relative to phosphine-containing arylpalladium(II) complexes previously studied, it has been possible to gain new insights into those steps that are common to the Heck reaction, namely, olefin insertion and  $\beta$ -hydride elimination. The present results show that there are notable differences in reactivity between arylpalladium(II) intermediates generated by decarboxylative palladation and those produced in conventional Heck reactions. Specifically, we have found that more electron-rich alkenes react preferentially with an arylpalladium(II) trifluoroacetate intermediate formed by decarboxylative palladation, whereas an opposite trend is found in conventional Heck reactions. In addition, we have found that the aralkylpalladium(II) trifluoroacetate intermediates that are formed upon olefin insertion in the present study are stabilized with respect to  $\beta$ -hydride elimination as compared to the corresponding phosphine-ligated aralkylpalladium(II) complexes. We have also crystallographically characterized an aralkylpalladium(II) trifluoroacetate intermediate derived from arylpalladium(II) insertion into norbornene, and this structure, too, contains an *S*-bound dimethyl sulfoxide ligand; the ipso-carbon of the transferred aryl group and trifluoroacetate function as the third and fourth ligands in the observed distorted square-planar palladium(II) complex.

## Introduction

The Heck coupling of alkenes with aryl halides is of fundamental importance in synthetic organic chemistry and has provided the inspiration for the development of many procedural variants as well as entirely different palladium-catalyzed coupling processes (eq 1).<sup>1</sup> Recently, while searching for catalysts that would promote a decarboxylative coupling of arene carboxylic acids with any of several different potential coupling partners, we discovered a system that accomplished a Heck-like coupling of arene carboxylic acids with alkenes (eq 2).<sup>2</sup>



The method we developed employs a catalytic quantity of palladium(II) bis(trifluoroacetate) (0.2 equiv) and silver(I)

carbonate (2 equiv) as a base (and stoichiometric oxidant) in a mixed solvent of dimethyl sulfoxide (DMSO, 5% v/v) in *N,N*-dimethylformamide (DMF) and promotes the coupling of an arene carboxylic acid (1 equiv) with an alkene (1.5 equiv). The decarboxylative coupling reaction is efficient with various ortho-substituted arene carboxylic acids as substrates, and many olefins are suitable coupling partners, including cyclic  $\alpha,\beta$ -unsaturated ketones.<sup>3</sup> Although the method is not currently practical for large-scale synthesis due to the high loadings of silver and palladium that are required, the process is nonetheless of interest given the novelty of the chemistry involved. Like the Heck reaction, the decarboxylative coupling of arene carboxylic acids with alkenes forms a styrene derivative as product. As we will show, the two processes share common elementary steps in their late stages, but there are important differences as well. The most

(1) Recent reviews: (a) Beletskaya, I. P.; Cheprakov, A. V. *Chem. Rev.* **2000**, *100*, 3009–3066. (b) Whitcombe, N. J.; Hii, K. K.; Gibson, S. E. *Tetrahedron* **2001**, *57*, 7449–7476.

(2) Myers, A. G.; Tanaka, D.; Mannion, M. R. *J. Am. Chem. Soc.* **2002**, *124*, 11250–11251.

(3) Tanaka, D.; Myers, A. G. *Org. Lett.* **2004**, *6*, 433–436.

noteworthy of these is the mechanism of generation of the arylpalladium(II) intermediate; in the Heck reaction this involves oxidative insertion of palladium(0) into a carbon–halogen bond, whereas in the decarboxylative coupling the process is mediated by palladium(II) and involves decarboxylative C–C bond cleavage. Here, we describe detailed mechanistic studies that shed light on each step of the decarboxylative coupling process.

**Development of a Stoichiometric System for Mechanistic Study.** To develop a system that was suitable for spectroscopic analysis of the organopalladium intermediates that are formed during the decarboxylative olefination reaction, we modified our standard conditions in several ways. First, a stoichiometric quantity of palladium(II) bis(trifluoroacetate) was used rather than 20 mol % as before,<sup>2</sup> obviating the need for an oxidant in the reaction. Second, the reaction was conducted in a stepwise fashion, either by lowering the reaction temperature or by withholding the olefinic coupling partner. This allowed us to observe intermediates that were present prior to the olefin insertion step (vide infra). It was found to be more convenient to use pure DMSO for spectroscopic studies rather than the mixed solvent previously employed (5% v/v DMSO in DMF). This had the added benefit of producing exceptionally clean spectra relative to those obtained from mixed solvent systems. Finally, in the absence of the olefinic substrate and the base (silver(I) carbonate), we found that partial protonolysis of an observed arylpalladium(II) trifluoroacetate intermediate (vide infra) occurred; however, this side reaction was completely suppressed when the sodium salt of the arene carboxylic acid was used as substrate. Our primary substrate for study was sodium 2,4,5-trimethoxybenzoate (**1**), selected on the basis of the simplicity of the <sup>1</sup>H NMR spectra of its derivatives, as well as its favorable reactivity profile.

## Results

**Spectroscopic Analysis of Carboxyl Exchange: Step 1.** <sup>1</sup>H NMR spectroscopic analysis of sodium 2,4,5-trimethoxybenzoate (**1**) in pure DMSO-*d*<sub>6</sub> showed two singlets in the aromatic region ( $\delta_{\text{H}}$  6.49 and 6.99, Figure 1a). These were shifted to lower field and were somewhat broadened upon addition of 1.2 equiv of palladium(II) bis(trifluoroacetate) at 23 °C ( $\delta_{\text{H}}$  6.62 and 7.01, major species, Figure 1b), which we attribute to the formation of trifluoroacetato palladium(II) 2,4,5-trimethoxybenzoate (**2**). In addition, a minor species was observed, characterized by a slight downfield shifting of the lower-field peak.<sup>4</sup> We assign the minor species as palladium(II) bis(2,4,5-trimethoxybenzoate) (**3**,  $\delta_{\text{H}}$  6.62 and 7.04, the distribution of major and minor products was ~6:1, Figure 1b). The structural assignments of the major and minor species are supported by the observation that the integration values of the two peaks were dependent upon the ratio of arene carboxylate to palladium(II) bis(trifluoroacetate). Thus, with 1.5 equiv of sodium 2,4,5-trimethoxybenzoate (**1**) relative to palladium(II) bis(trifluoroacetate) the ratio of trifluoroacetato palladium(II) 2,4,5-trimethoxybenzoate (**2**) to

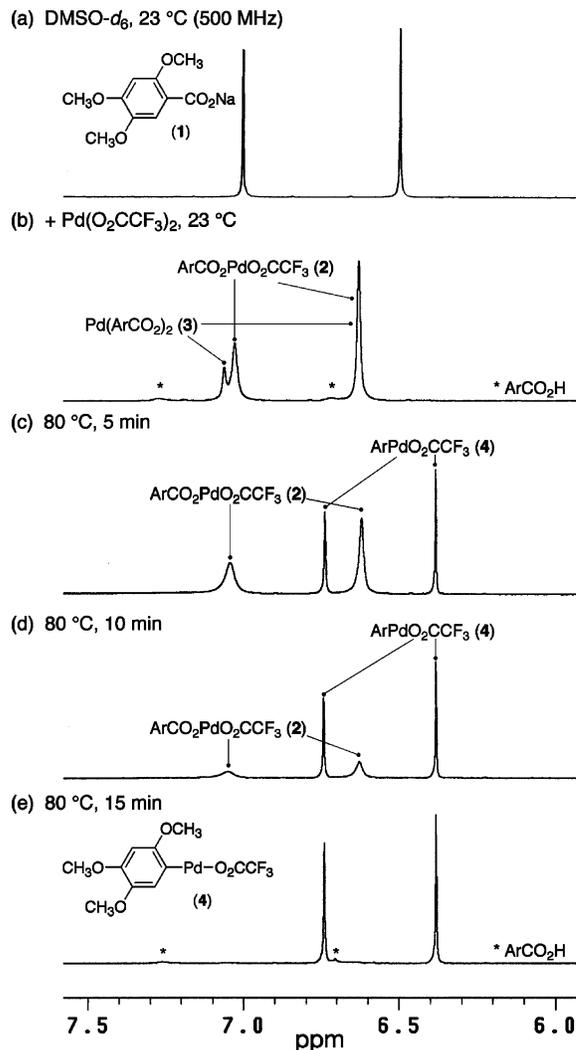


**Figure 1.** <sup>1</sup>H NMR study of the reaction between palladium(II) bis(trifluoroacetate) and sodium 2,4,5-trimethoxybenzoate (**1**) in the absence of an olefinic reactant. (a) <sup>1</sup>H NMR spectrum of sodium 2,4,5-trimethoxybenzoate (**1**) in DMSO-*d*<sub>6</sub> at 23 °C (500 MHz). (b) <sup>1</sup>H NMR spectrum 5 min after addition of Pd(O<sub>2</sub>CCF<sub>3</sub>)<sub>2</sub> at 23 °C. (c–e) <sup>1</sup>H NMR spectra after 5, 10, and 15 min heating, respectively, at 80 °C. Ar = 2,4,5-trimethoxyphenyl. Although not identified unambiguously, the peaks at  $\delta_{\text{H}}$  7.27 and 6.71 (labeled \*) correspond exactly with those observed in <sup>1</sup>H NMR analysis of a sample of 2,4,5-trimethoxybenzoic acid in DMSO-*d*<sub>6</sub> prepared independently.

palladium(II) bis(2,4,5-trimethoxybenzoate) (**3**) was ~1:1, while with 0.33 equiv of the sodium carboxylate the observed ratio was >95:5 (the initial concentration of palladium(II) bis(trifluoroacetate) was the same in both experiments). The product species were shown to be in dynamic equilibrium by variable-temperature <sup>1</sup>H NMR analysis (coalescence temperature ~40 °C). At 80 °C, where equilibrium is rapid on the <sup>1</sup>H NMR time scale, the downfield resonances were merged, appearing as a single peak (Figure 1c). Saturation-transfer experiments conducted at 20 °C established that the palladium(II) carboxylate species were exchanging even at ambient temperature.

**Observation and Structural Analysis of an Arylpalladium(II) Trifluoroacetate Intermediate; Palladium-Induced Decarboxylation: Step 2.** When solutions of the proposed trifluoroacetato palladium(II) 2,4,5-trimethoxybenzoate intermediate (**2**) in DMSO-*d*<sub>6</sub> were warmed to 80 °C, a smooth first-order transformation was observed ( $k = 4.8 \times 10^{-3} \text{ s}^{-1}$ ,  $t_{1/2} =$

(4) The presence of a third species is inferred from the large line width of the major, downfield aromatic peak in the <sup>1</sup>H NMR spectrum ( $\delta_{\text{H}}$  7.01,  $\Delta\nu_{1/2} = 8.1 \text{ Hz}$ ) and from the line shape of the carboxyl peaks in the <sup>13</sup>C NMR spectrum generated using <sup>13</sup>C-1 (carboxyl labeled, Figure 3a). The third species constitutes <15% of the reaction mixture (determined from deconvolution analysis of the <sup>13</sup>C NMR spectrum) and, considering the coincidence of the <sup>1</sup>H NMR chemical shifts, is presumably very close in structure to trifluoroacetato palladium(II) 2,4,5-trimethoxybenzoate (**2**), perhaps containing an *O*-bound rather than *S*-bound DMSO ligand or ligands.

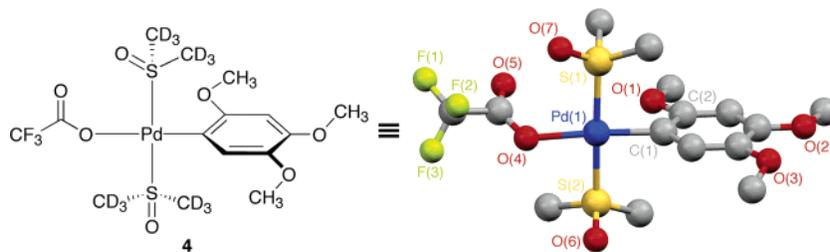


**Figure 2.** Structure of the arylpalladium(II) trifluoroacetate intermediate **4** as determined by X-ray crystallographic characterization. The unit cell also contains a molecule of DMSO- $d_6$ , which has been omitted here for clarity. Selected bond lengths (Å) and bond angles (deg): Pd(1)–S(1) 2.2805(9), Pd(1)–S(2) 2.2940(9), Pd(1)–O(4) 2.120(2), Pd(1)–C(1) 1.994(3); S(1)–Pd(1)–C(1) 88.27(9), S(2)–Pd(1)–C(1) 90.14(9), O(4)–Pd(1)–C(1) 173.99(13).

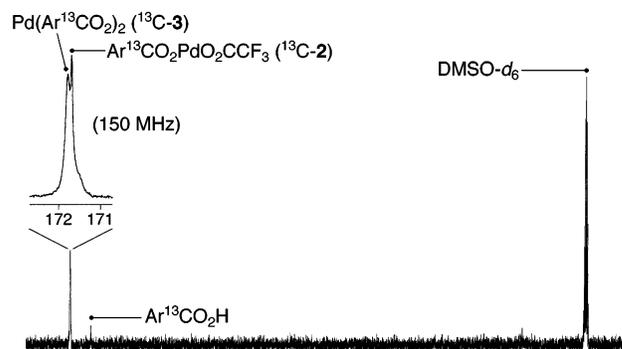
**Table 1.** Crystal Data and Structure Refinement Parameters for Arylpalladium(II) Trifluoroacetate **4**

Compound	<b>4</b>
empirical formula	$C_{17}H_{17}D_{12}F_3O_8PdS_3$
formula weight	633.05
temperature	193(2) K
crystal system	triclinic
space group	$P\bar{1}$ (2)
crystal color	yellow
unit cell dimensions	$a = 8.5349(16)$ Å, $\alpha = 77.006(4)^\circ$ $b = 12.272(2)$ Å, $\beta = 84.234(4)^\circ$ $c = 12.397(2)$ Å, $\gamma = 75.749(4)^\circ$
volume	$1224.9(4)$ Å <sup>3</sup>
Z	2
goodness-of-fit on $F^2$	0.930
final R indices [ $I > 2\sigma(I)$ ]	R1 = 0.0417, wR2 = 0.0664

2.5 min at 80 °C,  $^1H$  NMR analysis), producing the proposed arylpalladium(II) trifluoroacetate intermediate **4** (Figure 1c–e). Intermediate **4** was characterized by a substantial upfield shifting of the two singlets in the aromatic region ( $\delta_H$  6.40 and 6.72), as well as by a decrease in the line width of these peaks relative to the precursor (**4**:  $\delta_H$  6.72,  $\Delta\nu_{1/2} = 2.5$  Hz; **2**:  $\delta_H$  7.01,  $\Delta\nu_{1/2} = 8.1$  Hz). The decarboxylation reaction was complete after just 15 min at 80 °C, affording a product spectrum that was remarkably clean (Figure 1e).

Addition of tetrahydrofuran (THF) to a solution of the arylpalladium(II) trifluoroacetate intermediate **4** in DMSO- $d_6$  followed by cooling produced single crystals suitable for X-ray analysis. The structure of the crystalline product was determined to be *trans*-[(2,4,5-trimethoxyphenyl)Pd(DMSO- $d_6$ )<sub>2</sub>(O<sub>2</sub>CCF<sub>3</sub>)] (**4**, Figure 2, Table 1). The complex is monomeric and contains two DMSO- $d_6$  ligands, each bound to palladium through its sulfur atom (palladium–sulfur bond distances: 2.281 and 2.294 Å). The ipso-carbon–palladium bond distance is 1.994 Å, and the aryl ring is perpendicular to the palladium square plane ( $\angle$ S(1)–Pd(1)–C(1)–C(2) = 89.6°). Dissolution of the crystalline material in DMSO- $d_6$  and  $^1H$  NMR analysis of the resulting solution provided a spectrum that was identical to those obtained prior to crystallization; further, this solution was found to react with *tert*-butyl acrylate at 23 °C, affording *tert*-butyl 2,4,5-

(a)  $^{13}C$ -**1** + Pd(O<sub>2</sub>CCF<sub>3</sub>)<sub>2</sub>, DMSO- $d_6$ , 23 °C ( $^{13}C$  NMR, 100 MHz)



(b) 60 °C, 8 min

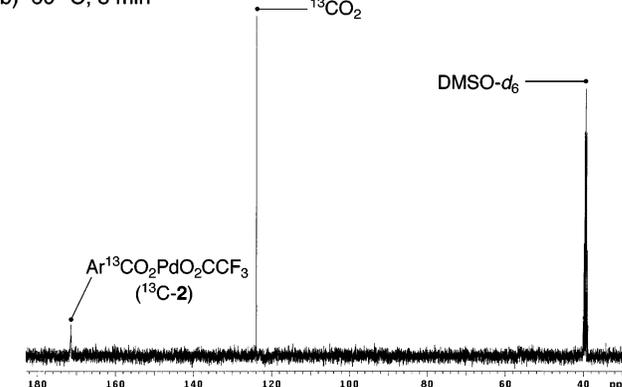


**Figure 3.**  $^{13}C$  NMR study of the decarboxylation of  $^{13}C$ -carboxyl 2,4,5-trimethoxybenzoate ( $^{13}C$ -**1**). (a)  $^{13}C$  NMR spectrum of  $^{13}C$ -**1** and Pd(O<sub>2</sub>CCF<sub>3</sub>)<sub>2</sub> in DMSO- $d_6$  at 23 °C (100 MHz, inset = 150 MHz). (b)  $^{13}C$  NMR spectrum after 8 min heating at 60 °C.

trimethoxycinnamate and palladium black (vide infra). These observations support the proposal that the arylpalladium(II) trifluoroacetate complex **4** is an intermediate in the decarboxylative olefination reaction.

The decarboxylative palladation reaction that produced the arylpalladium(II) trifluoroacetate complex **4** was also monitored by  $^{13}C$  NMR analysis using substrate bearing a  $^{13}C$ -label on the carboxyl carbon ( $^{13}C$ -**1**, Figure 3). When  $^{13}C$ -**1** and palladium(II) bis(trifluoroacetate) (1.2 equiv) were combined in DMSO- $d_6$  at 23 °C, we observed the carboxyl carbon resonance as a broad peak at  $\delta_C \approx 172$  ( $^{13}C$  NMR, 100 MHz). At higher field (150 MHz, see inset, Figure 3a), two partially resolved peaks were observed at  $\delta_C$  171.7 and 171.8, and these we tentatively assign as trifluoroacetato palladium(II) 2,4,5-trimethoxybenzoate (**2**) and palladium(II) bis(2,4,5-trimethoxybenzoate) (**3**), respectively, on the basis of the correspondence of their relative intensities with those observed in  $^1H$  NMR

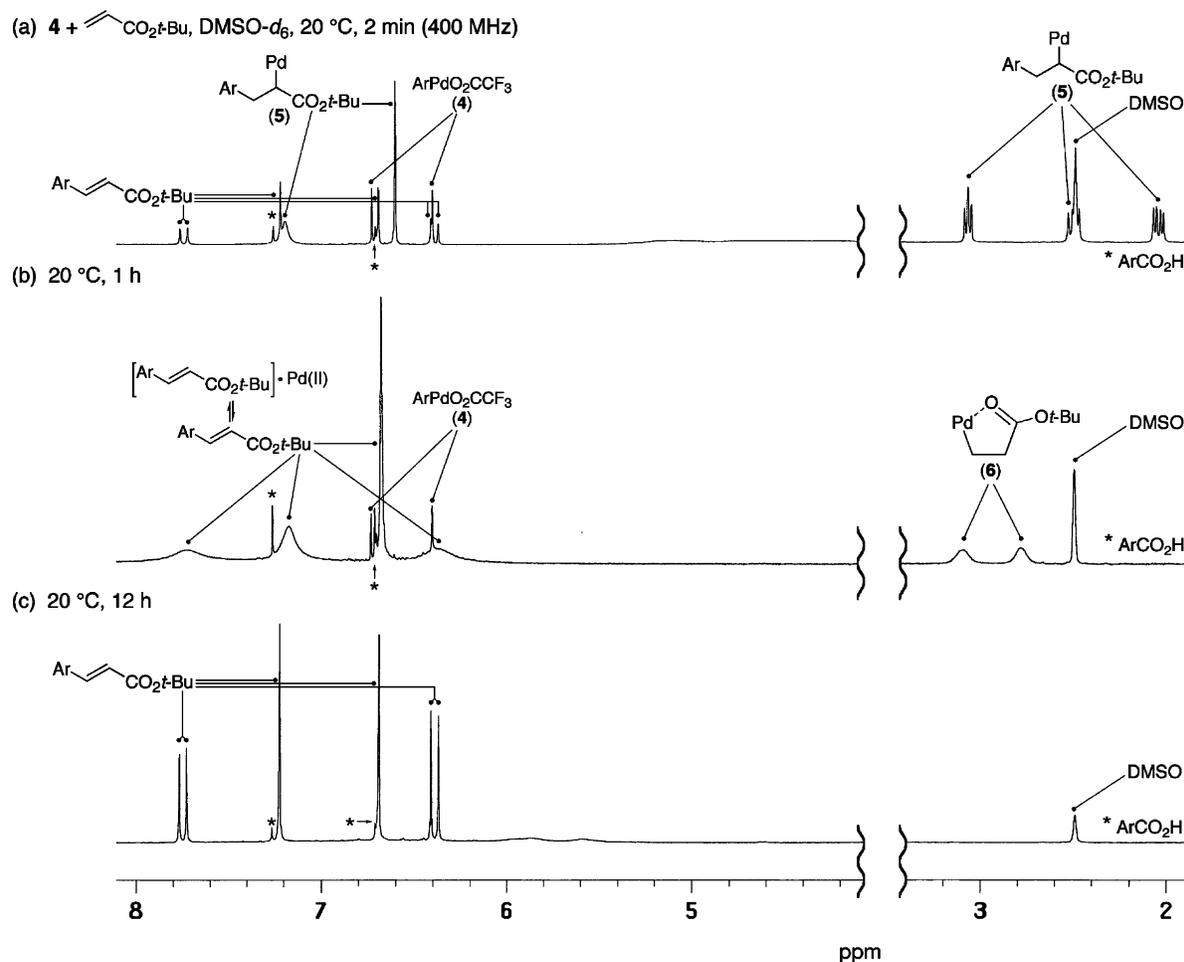


**Figure 4.**  $^1\text{H}$  NMR study of the olefin insertion reaction between *tert*-butyl acrylate and the arylpalladium(II) trifluoroacetate intermediate **4** and the subsequent  $\beta$ -hydride elimination reaction of the derived  $\sigma$ -alkylpalladium(II) intermediate (**5**). (a)  $^1\text{H}$  NMR spectrum 2 min after the addition of *tert*-butyl acrylate to a solution of arylpalladium(II) intermediate **4** in  $\text{DMSO-}d_6$  at  $20\text{ }^\circ\text{C}$  (400 MHz). (b)  $^1\text{H}$  NMR spectrum after 1 h at  $20\text{ }^\circ\text{C}$ . (c)  $^1\text{H}$  NMR spectrum after 12 h at  $20\text{ }^\circ\text{C}$ . Ar = 2,4,5-trimethoxyphenyl. Although not identified unambiguously, the peaks at  $\delta_{\text{H}}$  7.27 and 6.71 (labeled \*) correspond exactly with those observed in  $^1\text{H}$  NMR analysis of a sample of 2,4,5-trimethoxybenzoic acid in  $\text{DMSO-}d_6$  prepared independently.

analysis (see Figure 1b).<sup>4</sup> When warmed to  $60\text{ }^\circ\text{C}$ , the solution was found to smoothly evolve  $^{13}\text{C}$ -labeled carbon dioxide ( $\delta_{\text{C}}$  123.9),<sup>5</sup> while the peaks at  $\delta_{\text{C}} \approx 172$  diminished correspondingly (Figure 3b).<sup>6</sup> There is little doubt that the species giving rise to the newly formed peak is carbon dioxide, for degassing of the NMR sample removed it; also, we had earlier observed that decarboxylative palladation of 2,4,5-trimethoxybenzoic acid under our standard conditions led to a positive limewater test for carbon dioxide in the reaction effluent.<sup>2</sup>

Finally, we briefly note a series of observations concerning the influence of additives and solvent composition upon the rate of decarboxylative palladation, which bear upon mechanistic discussions later. First is the fact that added sodium trifluoroacetate (0–32 equiv) was found to slow the rate of decarboxylative palladation of **1** only slightly, even when in large excess ( $k = 1.5 \times 10^{-3}\text{ s}^{-1}$ , 32 equiv of  $\text{NaO}_2\text{CCF}_3$ , versus  $k = 4.8 \times 10^{-3}\text{ s}^{-1}$ , 0 equiv,  $^1\text{H}$  NMR analysis,  $80\text{ }^\circ\text{C}$ ), whereas addition of just 1.1 equiv of lithium bromide or tetra-*n*-butylammonium bromide completely abolished the decarboxylative palladation

reaction. Solutions with added bromide showed no evidence of decarboxylation nor of arylpalladium(II) intermediate formation even after heating at  $80\text{ }^\circ\text{C}$  for 2 h ( $^1\text{H}$  NMR analysis); the spectra were, however, consistent with the formation of a (nonreactive) 2,4,5-trimethoxybenzoato palladium(II) bromide intermediate (see Supporting Information). Last, the rate of decarboxylation was dependent upon the composition of the solvent, with the rate of reaction in a 19:1 mixture of  $\text{DMF-}d_7$  and  $\text{DMSO-}d_6$  being 2-fold greater than that in neat  $\text{DMSO-}d_6$  ( $k = 1.2 \times 10^{-3}\text{ s}^{-1}$ , 19:1 mixture of  $\text{DMF-}d_7$  and  $\text{DMSO-}d_6$ , versus  $k = 5.5 \times 10^{-4}\text{ s}^{-1}$ ,  $\text{DMSO-}d_6$ ,  $^1\text{H}$  NMR analysis,  $60\text{ }^\circ\text{C}$ ).

#### Observation of $\sigma$ -Alkylpalladium(II) Intermediates: Olefin Insertion and $\beta$ -Hydride Elimination: Steps 3 and 4.

Preformed solutions of the arylpalladium(II) trifluoroacetate intermediate **4** in  $\text{DMSO-}d_6$  or, in the case of low-temperature reactions ( $<20\text{ }^\circ\text{C}$ ), a 19:1 mixture of  $\text{DMF-}d_7$  and  $\text{DMSO-}d_6$ , respectively, were treated with 1.2 equiv of either *tert*-butyl acrylate, styrene, or acrylonitrile, and the ensuing reactions were followed by  $^1\text{H}$  NMR spectroscopy. The coupling of **4** and *tert*-butyl acrylate was most conveniently monitored, at  $20\text{ }^\circ\text{C}$  (Figure 4). We observed that, over the course of the reaction, peaks corresponding to **4** gradually diminished while signals

(5) Williams, E. A.; Cargioli, J. D.; Ewo, A. *J. Chem. Soc., Chem. Commun.* **1975**, 366–367.

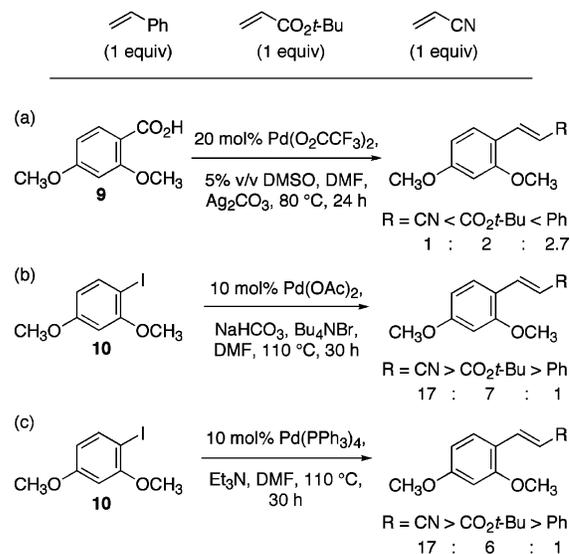
(6) The reaction was conducted at  $60\text{ }^\circ\text{C}$  rather than at  $80\text{ }^\circ\text{C}$  as in earlier  $^1\text{H}$  NMR experiments (Figure 1) to allow sufficient time to acquire  $^{13}\text{C}$  NMR spectra of intermediates in the reaction.

attributable to the  $\sigma$ -aryl palladium(II) intermediate **5** and *tert*-butyl 2,4,5-trimethoxycinnamate, the final product, grew in sequence (Figure 4).<sup>7</sup> After 1 h at 20 °C (Figure 4b), the intermediate **5** had been completely transformed into *tert*-butyl 2,4,5-trimethoxycinnamate; however, small amounts of the arylpalladium(II) trifluoroacetate intermediate **4** remained. In addition, the <sup>1</sup>H NMR spectrum was characterized by a distinctive broadening of peaks corresponding to the cinnamate ester. Significantly, the product spectrum at this point revealed a new and transient intermediate, characterized by two broad signals of equal intensity in the alkyl region ( $\delta_{\text{H}}$  2.78 and 3.10). This intermediate is proposed to be the palladacycle **6**, formed by (reversible) addition of a hydridopalladium(II) species to *tert*-butyl acrylate.<sup>8</sup> After 12 h at 20 °C (Figure 4c), palladium black had precipitated and peaks for the proposed palladacycle **6** were absent; further, peaks for *tert*-butyl 2,4,5-trimethoxycinnamate were notably sharp (yield ca. 90% by <sup>1</sup>H NMR) and the arylpalladium(II) trifluoroacetate intermediate **4** had been completely consumed. By conducting the olefin insertion reaction at 0 °C, the rate of  $\beta$ -hydride elimination was sufficiently slowed such that COSY, HMQC, and HMBC data could be obtained (data not shown); all supported the assignment of the primary intermediate as the  $\sigma$ -aryl palladium(II) species **5**. It is noteworthy that whereas in experiments employing 1.2 equiv of *tert*-butyl acrylate the olefinic peaks of both the substrate and the cinnamate product were observed to broaden as the reaction proceeded, in experiments employing 3.0 equiv of *tert*-butyl acrylate, the olefinic peaks of the cinnamate product appeared as sharp doublets throughout the reaction. Also, under the latter conditions, the palladacycle **6** was not observed.

The addition of the arylpalladium(II) trifluoroacetate intermediate **4** to styrene was observed to be much faster than the corresponding reaction with *tert*-butyl acrylate and proceeded to completion within 2 min at 23 °C. By conducting the reaction at -20 °C, it was possible to observe signals corresponding to the aliphatic protons of the  $\sigma$ -aryl palladium(II) intermediate **7** (see Supporting Information). In contrast to the adducts derived from *tert*-butyl acrylate and styrene, the acrylonitrile-derived  $\sigma$ -aryl palladium(II) intermediate **8** was found to be slow to form (requiring 30 min at 23 °C for completion, see Supporting Information) but, once formed, the complex exhibited remarkable stability ( $t_{1/2}$  = 25 h, 23 °C, insensitive to air) permitting its characterization by HMQC, HMBC, and <sup>13</sup>C NMR spectroscopy (see Supporting Information for <sup>13</sup>C NMR). Unlike the reactions of **4** with *tert*-butyl acrylate and styrene, which afforded exclusively *trans* products, the reaction of **4** with acrylonitrile afforded a small amount of the *cis*-cinnamitrile product, although the *trans* isomer predominated (3:1 *trans*:*cis*, respectively).<sup>9</sup> Finally, although the reaction of **4** with styrene was at least 3 orders of magnitude more rapid than the reaction of **4** with acrylonitrile, addition of styrene to preformed solutions

**Scheme 1.** Summary of Competitive Olefination Experiments with Styrene, *tert*-Butyl Acrylate and Acrylonitrile (1 equiv each)<sup>a</sup>

Results of Competition Experiments Employing:



<sup>a</sup> (a) 20 mol % Pd(O<sub>2</sub>CCF<sub>3</sub>)<sub>2</sub>, 5% v/v DMSO, DMF, Ag<sub>2</sub>CO<sub>3</sub>, 80 °C, 24 h; (b) 10 mol % Pd(OAc)<sub>2</sub>, NaHCO<sub>3</sub>, Bu<sub>4</sub>NBr, DMF, 110 °C, 30 h; (c) 10 mol % Pd(PPh<sub>3</sub>)<sub>4</sub>, Et<sub>3</sub>N, DMF, 110 °C, 30 h.

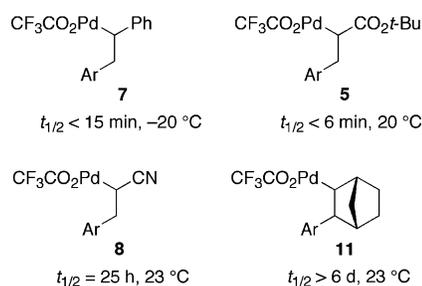


**Figure 5.** Half-lives of observed  $\sigma$ -aryl palladium(II) intermediates **5**, **7**, **8**, and **11**. In each case, the  $\sigma$ -aryl palladium(II) intermediate was transformed cleanly into the corresponding Heck-type product. Thus, the half-lives provide an estimation of the rate of  $\beta$ -hydride elimination in each case.

of the acrylonitrile-derived  $\sigma$ -aryl palladium(II) intermediate (**8**) gave exclusively cinnamitrile products.

**Competitive Olefination Experiments.** To confirm the relative reactivities of the olefinic substrates suggested by the individual experiments discussed above (styrene > *tert*-butyl acrylate > acrylonitrile), a competition experiment was conducted using our original catalytic decarboxylative olefination conditions and 1 equiv each of 2,4-dimethoxybenzoic acid (**9**) and the three olefins styrene, *tert*-butyl acrylate, and acrylonitrile (Scheme 1a). The product distribution was as expected, with the product stilbene > cinnamate > cinnamitrile (distribution: 2.7:2:1, respectively). Importantly, parallel competition experiments employing the Heck substrate 1-iodo-2,4-dimethoxybenzene (**10**) and, again, 1 equiv of each of the three olefins styrene, *tert*-butyl acrylate, and acrylonitrile under either the Jeffery conditions<sup>10</sup> (Scheme 1b) or using tetrakis(triphenylphosphine)palladium(0) (Scheme 1c) gave the opposite ordering of products (cinnamitrile > cinnamate > stilbene, 17:~7:1, respectively, in both cases).

**Structural Characterization of  $\sigma$ -Aryl palladium(II) Intermediates.** Each of the three  $\sigma$ -aryl palladium(II) inter-

(10) Jeffery, T. *Tetrahedron Lett.* **1994**, 35, 3051–3054.

(7) Peaks corresponding to unreacted *tert*-butyl acrylate (used in slight excess) are not observed in the spectrum at 2 min; however, broadened peaks are observed between  $\delta_{\text{H}}$  ca. 4.2–5.5 (Figure 4a). Similarly broadened peaks at  $\delta_{\text{H}}$  ca. 5.4–6.2 were observed at 12 h (Figure 4c). It is possible that these broadened peaks correspond to unreacted *tert*-butyl acrylate, shifted and broadened as a consequence of interaction with a Pd(II) species in solution.

(8) Brown, J. M.; Hii, K. K. *Angew. Chem., Int. Ed. Engl.* **1996**, 35, 657–659.

(9) Similar observations have been reported in conventional Heck reactions with acrylonitrile. Spencer, A. J. *Organomet. Chem.* **1984**, 270, 115–120.

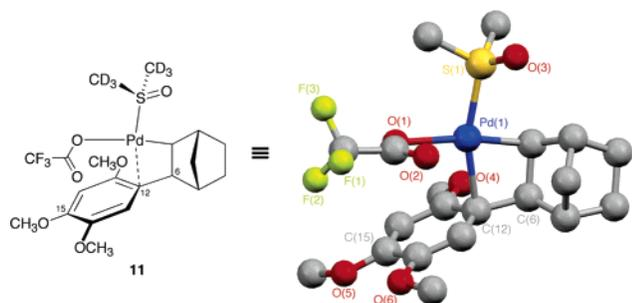


**Figure 6.** Structure of the norbornene adduct **11** as determined by X-ray crystallographic characterization. Selected bond lengths (Å) and bond angles (deg): Pd(1)–S(1) 2.2556(8), Pd(1)–O(1) 2.191(2), Pd(1)–C(5) 2.028(3), Pd(1)–C(12) 2.241(3); S(1)–Pd(1)–O(1) 95.35(7), C(15)–Pd(1)–C(12) 70.11(12).

mediates **5**, **7**, and **8** discussed above (see Figure 5) displayed fluxional behavior in  $^1\text{H}$  NMR analysis. For example, in  $^1\text{H}$  NMR analysis of the *tert*-butyl acrylate-derived intermediate **5** at 20 °C (Figure 4a) the resonance corresponding to the ortho-hydrogen resonance of the trimethoxyphenyl group was substantially broadened ( $\delta_{\text{H}}$  7.20,  $\Delta\nu_{1/2}$  = 11.1 Hz), whereas all other signals for this compound were sharp (e.g., for the meta-CH:  $\delta_{\text{H}}$  6.60,  $\Delta\nu_{1/2}$  = 2.3 Hz). The styrene-derived intermediate **7** exhibited similar behavior in  $^1\text{H}$  NMR analysis at –20 °C (see Supporting Information). For the acrylonitrile adduct **8**, the ortho-hydrogen resonance of the trimethoxyphenyl group was relatively sharp at 22 °C (5% v/v DMSO- $d_6$ /DMF- $d_7$ ,  $\delta_{\text{H}}$  7.34,  $\Delta\nu_{1/2}$  = 5.7 Hz); however, this signal was observed to broaden significantly as the probe temperature was reduced (–20 °C,  $\delta_{\text{H}}$  7.46,  $\Delta\nu_{1/2}$  37.8 Hz).<sup>11</sup> In each case, only the ortho-hydrogen resonance of the aryl ring was broadened in the  $^1\text{H}$  NMR spectrum. By contrast, the resonances for the hydrogens of the aliphatic carbons  $\alpha$  and  $\beta$  to the palladium appeared as sharp peaks.

The origin of the selective broadening observed in the  $^1\text{H}$  NMR spectra of the  $\sigma$ -aryl palladium(II) intermediates was made clear in experiments with a fourth alkene substrate, norbornene. Addition of norbornene (1.2 equiv) to a solution of the arylpalladium(II) trifluoroacetate intermediate **4** in DMSO- $d_6$  at 23 °C produced an observable  $\sigma$ -aryl palladium(II) intermediate (**11**) that displayed fluxional behavior in both  $^1\text{H}$  and  $^{13}\text{C}$  NMR analysis (see Supporting Information). As with the other alkene addition products we studied, fluxionality was associated solely with the trimethoxyphenyl group. Specifically, the ortho-hydrogen resonance of the norbornene adduct **11**, which was sharp in the  $^1\text{H}$  NMR spectrum at 23 °C (5% v/v DMSO- $d_6$ , DMF- $d_7$ ,  $\delta_{\text{H}}$  7.36,  $\Delta\nu_{1/2}$  = 6.4 Hz), became very broad upon cooling the probe to –20 °C ( $\delta_{\text{H}}$  7.41,  $\Delta\nu_{1/2}$  = 34.5 Hz), and the ipso-carbon was observed as a very broad peak at  $\delta_{\text{C}}$  ca. 80 in the  $^{13}\text{C}$  NMR spectrum at 20 °C. It is noteworthy that the ipso-carbon chemical shift appeared ca. 40 ppm upfield relative to that of *tert*-butyl 3-(2,4,5-trimethoxyphenyl)propionate, a palladium-free reference standard (ipso-C;  $\delta_{\text{C}}$  119.4). The norbornene-derived intermediate (**11**) was unusually stable. For example, only minor decomposition was observed after 6 days at 23 °C. Addition of THF and ethyl ether to a solution of **11** in DMSO- $d_6$  followed by cooling to –20 °C produced single crystals suitable for X-ray diffraction studies. The solid-state

**Table 2.** Crystal Data and Structure Refinement Parameters for  $\sigma$ -Aralkylpalladium(II) Trifluoroacetate **11**

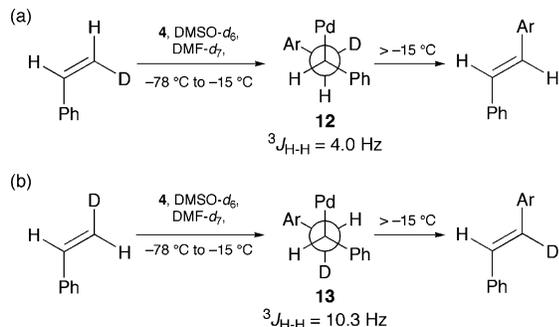
Compound	<b>11</b>
empirical formula	$\text{C}_{20}\text{H}_{21}\text{D}_6\text{F}_3\text{O}_6\text{PdS}$
formula weight	564.91
temperature	193(2) K
crystal system	orthorhombic
space group	$P2_12_1(19)$
crystal color	yellow
unit cell dimensions	$a = 9.3554(12)$ Å, $\alpha = 90^\circ$ $b = 14.1121(19)$ Å, $\beta = 90^\circ$ $c = 16.823(2)$ Å, $\gamma = 90^\circ$
volume	$2221.1(5)$ Å <sup>3</sup>
Z	4
goodness-of-fit on $F^2$	1.188
final $R$ indices [ $I > 2\sigma(I)$ ]	$R1 = 0.0330$ , $wR2 = 0.0689$

structure of the norbornene adduct (Figure 6, Table 2) shows that the palladium atom is bound to one molecule of DMSO (*S*-bound, palladium–sulfur bond distance = 2.256 Å), trifluoroacetate, a norbornyl carbon, and the ipso-carbon of the arene ring (palladium–carbon bond distance = 2.241 Å). The four ligands form a square-planar coordination environment for the palladium, somewhat distorted from an ideal geometry. In addition, the plane of the arene ring is canted relative to the C(6)–C(12) bond ( $\angle\text{C}(6)\text{--C}(12)\text{--C}(15)$  = 168.3°), but the two ortho-carbons are equidistant from the palladium atom (*o*-COCH<sub>3</sub>, 2.798 Å; *o*-CH, 2.803 Å).

**Stereochemical Course of Olefin Insertion and  $\beta$ -Hydride Elimination Steps.** By using *cis*- and *trans*- $\beta$ -deuterio-styrenes as olefinic coupling partners, we were able to determine the stereochemistry of both the olefin insertion and  $\beta$ -hydride elimination steps. Thus, reaction of the arylpalladium(II) trifluoroacetate intermediate **4** with *cis*- $\beta$ -deuterio-styrene gave unlabeled *trans*-2,4,5-trimethoxystilbene as the sole product (Scheme 2a), whereas reaction of **4** with *trans*- $\beta$ -deuterio-styrene gave *trans*- $\alpha$ -deuterio-2,4,5-trimethoxystilbene exclusively (Scheme 2b). By conducting low-temperature NMR experiments, it was possible to observe the intermediate  $\sigma$ -aryl palladium(II) complexes in each case. Thus, addition of **4** to *cis*- $\beta$ -deuterio-styrene at –40 °C produced the  $\sigma$ -aryl palladium(II) intermediate **12**, which exhibited a three-bond coupling ( $^3J_{\text{H-H}}$ ) of 4.0 Hz between the aliphatic protons, consistent with the conformation depicted in Scheme 2a, whereas addition of **4** to *trans*- $\beta$ -deuterio-styrene at –40 °C produced the  $\sigma$ -aryl palladium(II) intermediate **13**, which exhibited a 10.3-Hz coupling between the aliphatic protons, consistent with the conformation shown in Scheme 2b. These data are fully consistent with syn-addition and syn-elimination mechanisms in the olefin insertion and reductive elimination steps, respec-

(11) Full variable-temperature analysis was precluded by the thermal instability of the aralkylpalladium(II) intermediate and the freezing point of the solvent (5% v/v DMSO- $d_6$ , DMF- $d_7$ ).

**Scheme 2.**  $^1\text{H}$  NMR Studies Establishing the Stereochemical Course of the Olefin Insertion and  $\beta$ -Hydride Elimination Reactions of the  $\beta$ -D-Styrene Derivatives (a) *cis*- $\beta$ -D-Styrene and (b) *trans*- $\beta$ -D-Styrene<sup>a</sup>



<sup>a</sup> Ar = 2,4,5-trimethoxyphenyl. The non-alkyl ligands around palladium have been omitted for clarity.

tively, under the conditions of the decarboxylative olefination reaction.

## Discussion

The results of the experimental studies summarized in the paragraphs above support the primary features of the mechanism of the palladium-mediated decarboxylative olefination of arene carboxylic acids previously proposed,<sup>2</sup> while providing considerable additional detail with regard to the structures of intermediates in the process and the kinetics of their formation and breakdown. Using sodium 2,4,5-trimethoxybenzoate (**1** and  $^{13}\text{C}$ -**1**) as substrate and a stoichiometric quantity (1.2 equiv) of palladium(II) bis(trifluoroacetate) in  $\text{DMSO-}d_6$ , we readily monitored the stepwise process leading to decarboxylative insertion by  $^1\text{H}$  and  $^{13}\text{C}$  NMR spectroscopy (Figures 2 and 3). The data are consistent with an initial dynamic exchange of trifluoroacetate and the arene carboxylate substrate on the palladium(II) center. With just a slight excess of palladium(II) bis(trifluoroacetate) (1.2 equiv), the primary species in solution at 23 °C is believed to be trifluoroacetato palladium(II) 2,4,5-trimethoxybenzoate (**2**), with lesser amounts of palladium(II) bis(2,4,5-trimethoxybenzoate) (**3**) observable. The species were shown to be in equilibrium both by variable-temperature studies and by saturation-transfer experiments. We have tentative evidence for at least one other, minor species in solution which, if present, must correspond closely to the major species in solution, trifluoroacetato palladium(II) 2,4,5-trimethoxybenzoate (**2**), based upon the near identity of their chemical shifts.<sup>4</sup> In this regard, it is important to note that the complex of palladium(II) bis(trifluoroacetate) itself with DMSO was studied several years ago by Bancroft, Cotton, and Verbruggen.<sup>12</sup> The solid-state structure that they determined (Figure 7) showed that two DMSO molecules were bound to palladium(II) bis(trifluoroacetate) in *trans* fashion, with one *S*-bound and the other *O*-bound. Although the solid-state structures of the palladium(II) trifluoroacetate intermediates **4** and **11** presented here contain only *S*-bound DMSO ligands, it is evident from the work of Bancroft et al.<sup>12</sup> and from other crystal structures<sup>13</sup> that *O*-bound DMSO

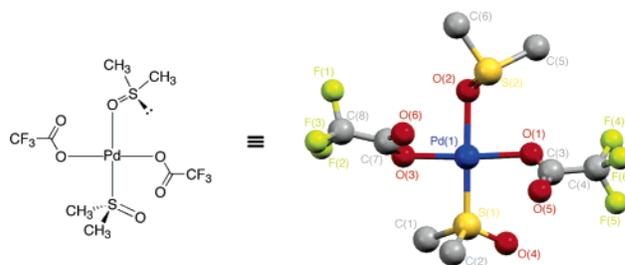
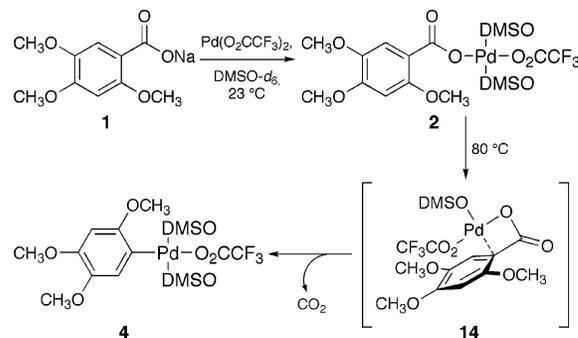


**Figure 7.** Structure of palladium(II) bis(trifluoroacetate) ligated by DMSO: *trans*-[(*O*-DMSO)(*S*-DMSO)Pd(O<sub>2</sub>CCF<sub>3</sub>)<sub>2</sub>].<sup>12</sup> Selected bond lengths (Å) and bond angles (deg): Pd(1)–S(1) 2.203(4), Pd(1)–O(2) 2.076(9), Pd(1)–O(1) 2.036(7), Pd(1)–O(3) 2.011(8); S(1)–Pd(1)–O(1) 91.9(3), S(1)–Pd(1)–O(3) 91.2(3), S(1)–Pd(1)–O(2) 174.9(2).

**Scheme 3.** Proposed Mechanism of Decarboxylative Palladation



complexes are viable and that dynamic processes of exchange between *S*- and *O*-bound forms must be considered as possible, if not likely, at every stage of the decarboxylative coupling process.<sup>14</sup> Also, we cannot rule out the presence of *cis*-palladium(II) intermediates.

The rate-determining step of the palladium-mediated decarboxylative coupling process is that where the C–C bond of the arene carboxylic acid is cleaved to form the crystallographically characterizable arylpalladium(II) trifluoroacetate intermediate **4** (Figures 1–3) and carbon dioxide (Figure 3). Under the conditions specified, decarboxylative palladation of substrate **1** occurs with a half-life of 2.5 min at 80 °C. The solid-state structure of the arylpalladium(II) trifluoroacetate intermediate **4** shows that the complex is *trans*-configured, with both DMSO ligands *S*-bound. Although many arylpalladium(II) complexes have been analyzed crystallographically, this is the only monodentate arylpalladium(II) trifluoroacetate known and only the second monodentate arylpalladium(II) species with dimethyl sulfoxide as a ligand.<sup>15</sup>

We propose that the formation of **4** from trifluoroacetato palladium(II) 2,4,5-trimethoxybenzoate (**2**) proceeds by the formation of a four-membered ring palladacyclic species such as **14**, depicted in Scheme 3, wherein the electrophilic palladium(II) center is bonded both to the arene carboxylate oxygen and the ipso-carbon of the arene ring, followed by extrusion of carbon dioxide and association of DMSO. Interesting and unresolved details of the process that transforms **2** into **4** are where dissociation and association of DMSO ligands occur, whether **14** is an energy minimum, and whether the DMSO molecules that remain bound to the palladium are coordinated

(12) Bancroft, D. P.; Cotton, F. A.; Verbruggen, M. *Acta Crystallogr., Sect. C* **1989**, *45*, 1289–1292.

(13) (a) Navarro-Ranninger, C.; López-Solera, I.; Alvarez-Valdés, A.; Rodríguez-Ramos, J. H.; Masaguer, J. R.; García-Ruano, J. L. *Organometallics* **1993**, *12*, 4104–4111. (b) Nonoyama, M.; Nakajima, K. *Polyhedron* **1999**, *18*, 533–543. (c) Johnson, B. F. G.; Puga, J.; Raithby, P. R. *Acta Crystallogr., Sect. B* **1981**, *37*, 953–956.

(14) Steinhoff, B. A.; Fix, S. R.; Stahl, S. S. *J. Am. Chem. Soc.* **2002**, *124*, 766–767.

(15) The other is benzyltriphenylphosphonium *cis*-[dichloro(2,4,6-trinitrophenyl)-(dimethyl sulfoxide-*S*)palladium(II)]: Vicente, J.; Arcas, A.; Borrachero, M. V. *J. Organomet. Chem.* **1989**, *359*, 127–137.

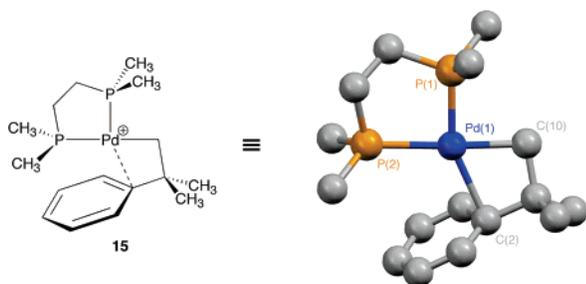


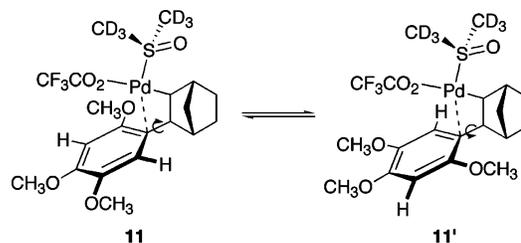
**Figure 8.** Structure of a  $\sigma$ -aryl palladium(II) intermediate **15** showing a  $\pi$ ,  $\eta^1$  palladium–arene interaction.<sup>17</sup> The counterion is tetrakis[3,5-bis(trifluoromethyl)phenyl]borate (BARF) and has been omitted for clarity. Selected bond lengths (Å) and bond angles (deg): Pd(1)–P(1) 2.220(2), Pd(1)–P(2) 2.363(2), Pd(1)–C(10) 2.065(7), Pd(1)–C(2) 2.343(6); P(1)–Pd(1)–P(2) 86.67(7), C(2)–Pd(1)–C(10) 66.2(3).

via sulfur or oxygen in transition structures.<sup>16</sup> At present we favor the pathway shown in Scheme 3 over a similar pathway involving a cationic organopalladium(II) intermediate (i.e., where a second DMSO ligand replaces trifluoroacetate in structure **14**). The fact that increasing proportions of DMSO slow the decarboxylative palladation reaction is consistent with the idea that dissociation of DMSO occurs prior to or during the rate-determining step, but the effect is not large ( $k = 1.2 \times 10^{-3} \text{ s}^{-1}$ , 19:1 mixture of DMF- $d_7$  and DMSO- $d_6$ , versus  $k = 5.5 \times 10^{-4} \text{ s}^{-1}$ , DMSO- $d_6$ ,  $^1\text{H}$  NMR analysis, 60 °C). Addition of trifluoroacetate was also observed to have a modest inhibitory effect upon the rate of decarboxylative palladation, but this is perhaps attributable to displacement of the equilibrium between palladium(II) bis(trifluoroacetate) and trifluoroacetato palladium(II) 2,4,5-trimethoxybenzoate (**2**) in the carboxyl-exchange step rather than loss of trifluoroacetate just prior to or during the transition state.

It is evident that trifluoroacetate plays a key role in the decarboxylative palladation reaction, for sources of palladium bearing other ligands (e.g., palladium(II) acetate, palladium(II) chloride, palladium(II) oxide, and palladium(II) triflate) were ineffective or gave inferior results in both catalytic and stoichiometric decarboxylation reactions, and added bromide completely inhibited decarboxylation, as discussed above. We believe that an electron-deficient palladium center is critical for decarboxylative palladation to occur. The fact that electron-rich arene carboxylic acids exhibit enhanced reactivity in decarboxylative palladation and the observation that electron-donating ligands such as phosphines and trialkylamines completely inhibit the reaction support this assertion.

With regard to the proposed formation and fragmentation of a four-membered palladacyclic intermediate, the work of Cámpora et al. must be cited, in which the crystallographically characterized cationic  $\sigma$ -aryl palladium(II) complex **15** (Figure 8, cf., the solid-state structure of **11**, Figure 6, and the proposed structure **14**, Scheme 3) was shown to extrude isobutene upon warming to 60 °C.<sup>17</sup> This extrusion was proposed to proceed

**Scheme 4.** Proposed Interconversion of Diastereomeric Complexes **11** and **11'**



by a fragmentation reaction that is isoelectronic with the extrusion of carbon dioxide proposed here. Finally, we note that the mechanism of decarboxylative palladation we propose is consistent with the observed regiochemistry of palladium substitution, where C–C bond formation in the subsequent olefination step is always to the ipso-carbon.<sup>18</sup>

Both of the final steps of the decarboxylative coupling process, olefin insertion and  $\beta$ -hydride elimination, were readily monitored by  $^1\text{H}$  NMR analysis of reaction mixtures prepared by the addition of an olefinic substrate (1.2 equiv) to preformed solutions of the arylpalladium(II) intermediate **4**. We followed the reactions of **4** with each of the olefins styrene, *tert*-butyl acrylate, and acrylonitrile. With each substrate, the rate of olefin insertion was greater than that of  $\beta$ -hydride elimination;  $\sigma$ -aryl palladium(II) intermediates were observed in all cases. The rates of olefin insertion into the palladium–carbon bond of the arylpalladium(II) trifluoroacetate intermediate **4** were found by direct measurement to be styrene > *tert*-butyl acrylate > acrylonitrile. The same ranking was also observed in the subsequent  $\beta$ -hydride elimination step from the derived  $\sigma$ -aryl palladium(II) intermediates. Although  $\beta$ -hydride elimination was found to be rate-determining (after decarboxylation to form **4**), the fact that addition of styrene to preformed solutions of the acrylonitrile-derived  $\sigma$ -aryl palladium(II) intermediate (**8**) gave only acrylonitrile-derived products suggests that olefin insertion is not reversible under the reaction conditions.

Results of a competition experiment using styrene, *tert*-butyl acrylate, and acrylonitrile (Scheme 1) are consistent with these observations; the product distribution was found to be stilbene > cinnamate ester > cinnamonnitrile, 2.7:2:1, respectively. By contrast, we observed that in similar competition experiments with the conventional Heck substrate 1-iodo-2,4-dimethoxybenzene, both under Jeffery conditions<sup>9</sup> or using tetrakis(triphenylphosphine)palladium(0), an inverse selectivity was observed (cinnamonnitrile > cinnamate ester > stilbene, 17:~7:1). In a prior study, Böhm and Herrmann showed that competitive couplings of aryl bromides with styrene and *n*-butyl acrylate using bis(tri-*ortho*-tolylphosphine)palladium(0) and related catalysts favored the cinnamate ester product under all conditions examined.<sup>19</sup> These results reveal a fundamental distinction in reactivity between the arylpalladium(II) intermediates formed by decarboxylative palladation and those formed in conventional Heck transformations. Again, we attribute this to the specialized ligand environment of the palladium(II) center, here, with reference to the olefin insertion and  $\beta$ -hydride elimination steps.

Detailed structural information for a  $\sigma$ -aryl palladium(II) intermediate formed during decarboxylative coupling was

(16) For other examples of the importance of DMSO as a solvent in Pd-catalyzed processes, see: (a) Larock, R. C.; Hightower, T. R. *J. Org. Chem.* **1993**, *58*, 5298–5300. (b) van Benethem, R. A. T. M.; Hiemstra, H.; Michels, J. J.; Speckamp, W. N. *J. Chem. Soc., Chem. Commun.* **1994**, 357–359. (c) Chen, M. S.; White, M. C. *J. Am. Chem. Soc.* **2004**, *126*, 1346–1347. (d) Zhou, C.; Larock, R. C. *J. Am. Chem. Soc.* **2004**, *126*, 2302–2303. (e) Fraunhoffer, K. J.; Bachovchin, D. A.; White, M. C. *Org. Lett.* **2005**, *7*, 223–226.

(17) Cámpora, J.; Gutiérrez-Puebla, E.; López, J. A.; Monge, A.; Palma, P.; del Río, D.; Carmona, E. *Angew. Chem., Int. Ed.* **2001**, *40*, 3641–3644.

(18) Some substrates lacking an ortho substituent undergo competitive ortho-palladation to form isocoumarin products; however, this transformation does not involve decarboxylation: (a) Miura, M.; Tsuda, T.; Satoh, T.; Pivsa-rt, S.; Nomura, M. *J. Org. Chem.* **1998**, *63*, 5211–5215. (b) See ref 2.

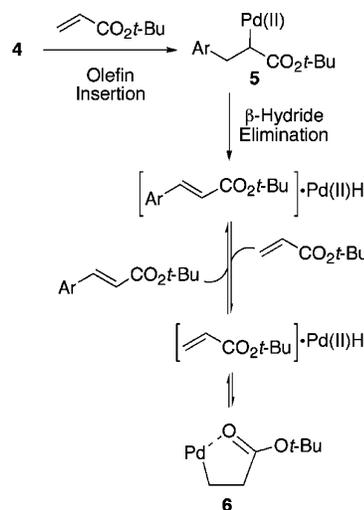
(19) Böhm, V. P. W.; Herrmann, W. A. *Chem.–Eur. J.* **2001**, *7*, 4191–4197.



obtained by investigation of the reaction of norbornene with the arylpalladium(II) trifluoroacetate intermediate **4**. In this case, the rate of olefin insertion was too rapid to measure conveniently by  $^1\text{H}$  NMR analysis at 23 °C (complete reaction <5 min). The  $\sigma$ -aryl palladium(II) insertion product (**11**) was formed in high yield and was crystallographically characterized (Figure 5). The solid-state structure clearly shows that the palladium atom is bound to the ipso-carbon of the arene ring in  $\eta^1$ -fashion.<sup>20</sup> The  $^{13}\text{C}$  NMR spectrum of **11** in solution revealed a pronounced upfield shifting of the ipso-carbon resonance. The solution NMR data are also consistent with exchange-induced broadening of the ortho-hydrogen resonance, which we attribute to equilibration between the diastereomeric ipso-bonded structures labeled as **11** and **11'** in Scheme 4. We also observed exchange-induced broadening of the ortho-hydrogen resonances in each of the  $\sigma$ -aryl palladium(II) intermediates derived from *tert*-butyl acrylate, styrene, and acrylonitrile (**5**, **7**, and **8**, respectively, Figure 5), but in these cases the ipso-carbon resonances were not markedly shifted relative to a palladium-free standard. Solid-state structures of several  $\sigma$ -aryl palladium(II) species have shown that the nature of the bonding between palladium and the ipso-carbon can vary between  $\eta^1$  and  $\eta^2$  in closely related systems.<sup>20b</sup> Also, the degree of upfield shifting of the ipso-carbon resonance in such complexes is highly variable. That the rigid norbornyl  $\sigma$ -aryl palladium(II) intermediate **11**, with enforced eclipsing interactions between the intervening carbon atoms that link the palladium and the arene ring, should display considerably greater upfield shifting of the ipso-carbon relative to that of the conformationally more mobile  $\sigma$ -aryl palladium(II) intermediates **5** and **8** is thus perhaps not surprising.

Previous studies of olefin insertion into arylpalladium(II) intermediates have been conducted primarily in the context of mechanistic studies of the Heck reaction, and in the few cases where  $\sigma$ -aryl palladium(II) intermediates were observed, these typically involved substrates that were incapable of  $\beta$ -hydride elimination.<sup>21</sup> A notable exception comes from the work of Brown and Hii,<sup>8</sup> where the  $\sigma$ -aryl palladium(II) intermediate derived from insertion of methyl acrylate into the arylpalladium bond of phenyl(bis(diphenylphosphino)ferrocene)palladium(II) triflate was observed to form rapidly at -60 °C. As in the present work, Brown and Hii observed that olefin insertion was faster than the subsequent  $\beta$ -hydride elimination. Their study provides a rare example of an observable phosphine-containing  $\sigma$ -aryl palladium(II) intermediate that is capable of  $\beta$ -hydride elimination (shown to be rapid above -40 °C in that system). In this regard, it is interesting to note that when we added an excess of triphenylphosphine to the relatively stable  $\sigma$ -aryl palladium(II) intermediate derived from acrylonitrile (**7**,  $t_{1/2}$  = 25 h, 23 °C),  $\beta$ -hydride elimination was complete within minutes at 23 °C.

**Scheme 5.** Plausible Sequence for the Formation of the Palladacycle **6** from the  $\sigma$ -Arylpalladium(II) Intermediate **5** (see ref 8)



The relative stabilities of the  $\sigma$ -aryl palladium(II) intermediates we observe (**5**, **7**, and **8**, Figure 5) suggest that  $\beta$ -hydride elimination is slowed by the presence of electron-withdrawing substituents on the  $\alpha$ -carbon. It is tempting to speculate that the same features of the palladium center and its ligand environment that promote the decarboxylative palladation reaction may also contribute to the stability of the  $\sigma$ -aryl palladium(II) intermediates we observe, as well as account for the fact that electron-rich olefins insert into the arene-palladium bond more rapidly than electron-poor olefins. The common feature would appear to be electron deficiency at the metal center.

Additional details of the olefin insertion and  $\beta$ -hydride elimination steps emerge from consideration of the data from the stepwise reaction of the arylpalladium(II) intermediate **4** with *tert*-butyl acrylate (Figure 4, Scheme 5). In this case, we observed that as the  $\sigma$ -aryl palladium(II) intermediate was transformed into the cinnamate ester product, a new and transient species was formed, which we assign as the palladacycle **6**. A very similar intermediate was identified by Brown and Hii in their studies of the Heck reaction cited above. They proposed a sequence for its formation that involved the coordination of *tert*-butyl acrylate to a hydridopalladium(II) species followed by olefin insertion to form the observed palladacyclic intermediate.<sup>8</sup> The formation of **6** as an intermediate in our system is reasonable, given that there was no base present in the reaction mixture. It also accounts for the fact that although the olefin insertion reaction was initially very rapid ( $t_{1/2}$  <5 min), even after 1 h a substantial amount of unreacted arylpalladium(II) trifluoroacetate intermediate **4** remained in solution (Figure 5b). At this point in the reaction (1 h, 23 °C, Figure 4b), all remaining *tert*-butyl acrylate (1.2 equiv was employed) had apparently been temporarily sequestered in the form of the palladacycle **6**. After 12 h at 23 °C (Figure 4c), however, neither the arylpalladium(II) trifluoroacetate intermediate **4** nor the palladacycle **6** remained, and complete conversion to the cinnamate ester (and palladium black) was achieved. We did not observe formation of the palladacycle **6** in the initial phase of the reaction (1.2 equiv of *tert*-butyl acrylate, 10 min, 23 °C, Figure 4a) nor at any point in the reaction when a large excess of *tert*-butyl acrylate was used (3.0 equiv). Also, at no point in the reaction

(20) (a) Li, C.-S.; Cheng, C.-H.; Liao, F.-L.; Wang, S.-L. *J. Chem. Soc., Chem. Commun.* **1991**, 710–712. (b) Catellani, M.; Mealli, C.; Motti, E.; Paoli, P.; Perez-Carreno, E.; Pregosin, P. S. *J. Am. Chem. Soc.* **2002**, *124*, 4336–4346 and references therein.

(21) Examples of NMR studies of  $\sigma$ -aryl palladium(II) intermediates in the Heck reaction: (a) Li, C.-S.; Jou, D.-C.; Cheng, C.-H. *Organometallics* **1993**, *12*, 3945–3954. (b) Hii, K. K.; Claridge, T. D. W.; Brown, J. M. *Angew. Chem., Int. Ed. Engl.* **1997**, *36*, 984–987. (c) Ludwig, M.; Strömberg, S.; Svensson, M.; Åkermark, B. *Organometallics* **1999**, *18*, 970–975. (d) Hahn, C.; Morvillo, P.; Vitagliano, A. *Eur. J. Inorg. Chem.* **2001**, 419–429. (e) Spaniel, T.; Schmidt, H.; Wagner, C.; Merzweiler, K.; Steinborn, D. *Eur. J. Inorg. Chem.* **2002**, 2868–2877. (f) Clique, B.; Fabritius, C.-H.; Couturier, C.; Monteiro, N.; Balme, G. *Chem. Commun.* **2003**, 272–273.

sequence did we observe any hydridopalladium(II) intermediate. Evidently, addition of palladium hydride to *tert*-butyl acrylate is both rapid and reversible in this system. Finally, we note that during the reaction of **4** with *tert*-butyl acrylate, peaks corresponding to the cinnamate ester product in the  $^1\text{H}$  NMR spectrum were broadened, which we attribute to dynamic association of the product with palladium(II) intermediates in solution. Later, when product formation was complete and palladium black had precipitated, we saw no such broadening. We also observed broadening of product peaks during  $^1\text{H}$  NMR monitoring of the reactions of **4** with styrene and acrylonitrile, which we attribute to dynamic association of the stilbene and cinnamionitrile product, respectively, with palladium(II) intermediates in solution.

One of the more unusual features of the (catalytic) decarboxylative coupling reaction is the fact that 2-cyclohexen-1-ones are viable olefinic coupling partners.<sup>3</sup> With such substrates, the  $\sigma$ -aryl palladium(II) adducts that would be expected to form (by syn-addition of the arylpalladium(II) intermediate to the enone) must undergo an apparent anti-elimination. Although reasonable mechanisms have been proposed that avoid invoking an anti  $\beta$ -hydride elimination step (e.g., stereoinversion via a palladium enolate intermediate),<sup>22</sup> we felt that it was important in the present study to ensure that olefin insertion and  $\beta$ -hydride elimination were occurring by the expected syn pathways.<sup>23</sup> As is evident from our experiments with *cis*- and *trans*- $\beta$ -deuteriostyrene (Scheme 2), both steps proceeded with complete syn-stereospecificity.

## Conclusions

In summary, we have presented NMR and X-ray crystallographic evidence for many of the proposed intermediates in a process leading to the decarboxylative olefination of arene carboxylic acids. The data are consistent with a reaction sequence involving carboxyl exchange between palladium(II) bis(trifluoroacetate) and an arene carboxylic acid substrate, decarboxylation to form an arylpalladium(II) trifluoroacetate intermediate, then olefin insertion and  $\beta$ -hydride elimination. The decarboxylation step is rate-determining and is proposed to involve intramolecular coordination of an electron-deficient palladium(II) center to the ipso-carbon of the arene ring followed by expulsion of carbon dioxide and formation of an arylpalladium(II) intermediate. Using the discrete, crystallographically characterized arylpalladium(II) trifluoroacetate intermediate **4**, prepared by decarboxylative palladation, we were able to monitor spectroscopically the ensuing olefin insertion and  $\beta$ -hydride elimination steps. Although these steps are nominally common to the Heck reaction, it is evident from the data that the organopalladium(II) intermediates of the present study exhibit reactivities that are different from those produced during conventional Heck couplings. Specifically, we observe that the arylpalladium(II) trifluoroacetate intermediate **4** couples preferentially with electron-rich olefins, whereas arylpalladium(II) species formed in conventional Heck reactions react preferen-

tially with electron-poor olefins. Also, we observed that the  $\sigma$ -aryl palladium(II) trifluoroacetate intermediates produced upon olefin insertion were stabilized relative to corresponding intermediates produced in Heck couplings. We believe that these differences are attributable to the electron-deficient nature of the palladium(II) species involved.

## Experimental Section

**2,4,5-Trimethoxyphenylpalladium(II) Trifluoroacetate (4).** A 4-mL screw-cap vial equipped with a Teflon-coated stir bar was charged with palladium(II) bis(trifluoroacetate) (24.0 mg, 0.0722 mmol, 1.2 equiv), sodium 2,4,5-trimethoxybenzoate (**1**, 14.1 mg, 0.0602 mmol, 1.0 equiv), and DMSO- $d_6$  (0.6 mL). An atmosphere of argon was introduced, and the vial was sealed. The sealed vial was heated at 80 °C for 10 min and then was allowed to cool to 23 °C. The cooled reaction solution was transferred to an NMR tube, an atmosphere of argon was introduced, the NMR tube was sealed, and the following spectroscopic data were recorded.  $^1\text{H}$  NMR (500 MHz, DMSO- $d_6$ ):  $\delta$  6.72 (s, 1H, *o*-CH), 6.39 (s, 1H, *m*-CH), 3.81 (s, 3H, OCH<sub>3</sub>), 3.71 (s, 3H, OCH<sub>3</sub>), 3.67 (s, 3H, OCH<sub>3</sub>);  $^{13}\text{C}$  NMR (100 MHz, DMSO- $d_6$ ):  $\delta$  158–160 (br, CF<sub>3</sub>CO<sub>2</sub>), 154.8, 147.5, 142.1 (3C, COCH<sub>3</sub>), 118.9 (*o*-CH), 114.7 (*i*-C), 97.9 (*m*-CH), 56.4, 56.2, 55.7 (3C, OCH<sub>3</sub>);  $\delta_{\text{F}}$  (376 MHz, DMSO- $d_6$ ): -73.1.

**A Typical Procedure for the Preparation of a  $\sigma$ -Aralkylpalladium(II) Intermediate (Experiments Conducted at or above 20 °C).** To a solution of the arylpalladium(II) trifluoroacetate intermediate **4** in DMSO- $d_6$  (0.6 mL) in a 4-mL screw-cap vial under an argon atmosphere, prepared as described above, was added an olefinic reactant (1.2 equiv) neat, via syringe. The vial contents were mixed, and the resulting solution was transferred to an NMR tube. An atmosphere of argon was introduced, the NMR tube was sealed, and the sealed tube was inserted into an NMR probe pre-equilibrated at the desired temperature. Spectroscopic data were then recorded.

**A Typical Procedure for the Preparation of a  $\sigma$ -Aralkylpalladium(II) Intermediate (Experiments Conducted below 20 °C).** A 4-mL screw-cap vial equipped with a Teflon-coated stir bar was charged with palladium(II) bis(trifluoroacetate) (24.0 mg, 0.0722 mmol, 1.2 equiv), sodium 2,4,5-trimethoxybenzoate (**1**, 14.1 mg, 0.0602 mmol, 1.0 equiv), and a solution of DMSO- $d_6$  in DMF- $d_7$  (5% v/v, 0.6 mL). An atmosphere of argon was introduced, and the vial was sealed. The vial was heated at 80 °C for 10 min and then was allowed to cool to ambient temperature (23 °C). The vial was further cooled to -40 °C, and an olefinic reactant (1.2 equiv) in DMF- $d_7$  (50  $\mu\text{L}$ ) was added via syringe. The vial contents were mixed, and the resultant solution was transferred to an NMR tube. An atmosphere of argon was introduced, and the NMR tube was sealed. The sealed tube was cooled to -78 °C (causing the sample solution to solidify), and then the NMR tube and its solid contents were transferred to an NMR probe pre-equilibrated to the desired temperature (-40 to 0 °C). The solid sample quickly liquefied, whereupon NMR data were recorded.

**X-ray Crystallography.** Crystal data and details of data collection for compounds **4** and **11** are given in Tables 1 and 2, respectively. In each case, a suitable crystal was chosen and mounted on a glass fiber using paratone. X-ray crystallographic data were collected using a Bruker SMART CCD-based diffractometer equipped with an Oxford Cryostream low-temperature apparatus operating at 193 K. Cell parameters were retrieved using SMART<sup>24</sup> software and were refined using SAINT<sup>25</sup> software. The structures were solved by the direct method using the SHELXS-97<sup>26</sup> program, and the data were refined

(22) (a) Friestad, G. K.; Branchaud, B. P. *Tetrahedron Lett.* **1995**, *36*, 7047–7050. (b) Adams, N. J.; Bargon, J.; Brown, J. M.; Farrington, E. J.; Galardon, E.; Giernoth, R.; Heinrich, H.; John, B. D.; Maeda, K. *Pure Appl. Chem.* **2001**, *73*, 343–346.  
(23) (a) Dieck, H. A.; Heck, R. F. *J. Am. Chem. Soc.* **1974**, *96*, 1133–1136. (b) Thorn, D. L.; Hoffmann, R. *J. Am. Chem. Soc.* **1978**, *100*, 2079–2090. (c) Larock, R. C.; Baker, B. E. *Tetrahedron Lett.* **1988**, *29*, 905–908.

(24) SMART, version 5.625 (NT); Bruker Analytical X-ray Systems: Madison, WI, 2001.  
(25) SAINT, version 6.22 (NT); Bruker Analytical X-ray Systems: Madison, WI, 2001.  
(26) Sheldrick, G. M. *SHELXS-90*; University of Göttingen: Göttingen, Germany, 1990.

by the least-squares method on  $F^2$ , SHELXL-97,<sup>27</sup> incorporated in SHELXTL-PC v 5.10.<sup>28</sup>

**Acknowledgment.** Financial support from the National Science Foundation is gratefully acknowledged. We thank Dr. Richard Staples for the X-ray analysis of compounds **4** and **11**.

(27) Sheldrick, G. M. *SHELXL-97*; University of Göttingen: Göttingen, Germany, 1997.

(28) *SHELXTL*, version 5.10 (PC version); Bruker Analytical X-ray Systems: Madison, WI, 1998.

D.T. acknowledges financial support from Dainippon Pharm. Co., LTD (Japan).

**Supporting Information Available:** Spectral data for compounds **1–5**, **7**, **8**, and **11–13** and X-ray crystallographic data (including thermal ellipsoid diagrams) for structures **4** and **11** (CIF, PDF). This material is available free of charge via the Internet at <http://pubs.acs.org>.

JA052099L